 CMES, vol.24, no.2, pp.123-141, 2008

Phonon Transport and Thermal Conductivity Percolation in Random Nanoparticle Composites

Weixue Tian[1] **and Ronggui Yang**[2]

Abstract: In this paper, we investigated the effective thermal conductivity of three dimensional nanocomposites composed of randomly distributed binary nanoparticles with large differences (contrast ratio) in their intrinsic (bulk) thermal conductivity. When random composites are made from particles with very different thermal conductivity (large contrast ratio), a continuous phase of high thermal conductivity constituent is formed when its volumetric concentration reaches beyond the percolation threshold. Such a continuous phase of material can provide a potentially low resistance pathway for thermal transport in random composites. The percolation theory predicts the thermal conductivity of the random composites to increase according to a scaling law with increasing concentration of the high thermal conductivity constituent after percolation. However, when the characteristic size of the particles in the nanocomposites is comparable to or smaller than the phonon mean free path, the phonon scattering at interfaces between two materials can introduce significant thermal resistance in the highly conductive phonon pathway. Such interfacial thermal resistance can reduce the thermal conductivity of the nanoparticle composites. The thermal conductivity of the random nanoparticle composites thus deviates significantly from the predictions of the percolation theory. In this study, the Monte Carlo simulation was employed to generate random distribution of nanoparticles and to simulate the phonon transport in random nanoparticle composites. The effects of particle size, thermal conductivity contrast ratio, and the phonon-interface scattering characteristics on the effective thermal conductivity of random nanoparticle composites are scrutinized. The effective thermal conductivity of the random nanoparticle composites are mainly controlled by the interface density (interfacial area per unit volume) in the composites. The percolating pathway formed by the high thermal conductivity constituents is not as effective in improving the thermal conductivity of the random nanoparticle composites for a wide range of volumetric concentrations compared to a random composite with larger particle dimensions. Similarly, the thermal conductivity contrast ratio of the constituents only plays a limited role in determining the thermal conductivity of the composites studied. This study can be important in studying flexible thermoelectric materials and thermal interface materials.

Keyword: nanocomposite, thermal conductivity, percolation theory, phonon transport, Monte Carlo simulation

1 Introduction

Nanocomposites are finding important applications in many emerging technologies such as high efficiency thermoelectric devices [Dresselhaus et al (2007), Hsu et al (2004), Heremans et al (2005)], thermal management system [Xu and Fisher (2006), Huang et al (2005)], dye-sensitized solar cells [Oregan and Gratzel (1991)] and among others due to the abundant existence of interfaces and their unique transport properties. Studies over the past on periodic semiconductor nanowire and nanoparticle composites composed of materials with intrinsic thermal conductivity on the same order of magnitude showed that the ther-

[1] Department of Mechanical Engineering, University of Colorado, Boulder, CO, USA, currently at Caterpillar Champaign Simulation Center, Champaign, IL, USA

[2] Department of Mechanical Engineering, University of Colorado, Boulder, CO, USA, Email: Ronggui.Yang@Colorado.Edu

mal conductivity of the nanocomposites is significantly smaller than that of their bulk counterparts due to phonon-interface scattering [Yang and Chen, (2004), Yang et al (2005), Prasher (2006), Tian and Yang (2007a)]. Such a thermal conductivity reduction is an important bless for thermoelectric materials where the figure of merit (ZT) is defined as $ZT = \frac{S^2\sigma T}{k}$, in which S, σ, k and T are the Seebeck coefficient, electrical conductivity, thermal conductivity, and absolute temperature, respectively [Goldsmid (1964)]. Thermoelectric nanocomposites are thus expected to play a more significant role in thermal management and power generation using waste heat and solar energy [Tritt and Subramanian (2006)].

Material research community has long been interested in developing multifunctional materials by tailoring the existing properties of constituents with large contrast ratio. One of the typical examples is the efforts in developing nanostructured thermal interface materials using high thermal conductivity fillers such as metallic particles and carbon nanotubes [Hu et al (2004), Xu and Fisher (2006)]. Several commonly used fabrication techniques such as hot pressing [Kusunose et al (2005)] or spark plasma sintering [Zhan et al (2003)] tend to produce nanocomposites with random structures. Clustering of particles and wires often occurs in these random composites. When particles or wires with high transport properties [thermal conductivity or electrical conductivity] are randomly dispersed in a matrix material with low transport properties, the largest cluster can form a percolation network [Stauffer and Aharony (1991)]. That says, the largest cluster of highly conductive material can connect the opposite boundaries when the volumetric concentration of high conductivity materials reaches certain limit. This limit of volumetric concentration, defined as the percolation threshold, is determined by the geometric characteristics of particles or wires. The percolating network can potentially create a low resistance pathway for transport between these opposite boundaries and the conductivity of the composites thus increases significantly with volumetric concentration after percolation. Percolation theory predicts that the conductivity of composites near the percolation threshold obeys the scaling law, i.e.$\sigma \propto (\Phi - \Phi_c)^t$, where σ is the conductivity of the composite, Φ is the volumetric concentration of the conductor, Φ_c is the percolation threshold and t is a conductivity exponent which does not depend on the lattice geometry but on the dimension [Stauffer and Aharony (1991)]. More rigorous discussion of the percolation theory and its prediction on conduction properties can be found elsewhere [Stauffer and Aharony (1991), Kirkpatrick (1973)]. Although its predictions for electrical conductivity have been confirmed by several experiments [Last and Thouless (1971), Dubson and Garland (1985)], the percolation theory remains largely a geometrical and empirical theory, in which many factors in real composite materials such as the interface resistance, particle size or material property contrast can not be easily incorporated. For example, both the percolation threshold and conductivity exponent for the electrical conductivity of metallic nanoparticle composites were found to deviate from the conventional percolation theory because of particle aggregation and various electrical contact resistance [Gonon and Boudefel (2006), Yamamuro et al (1999)]. The electrical conductivity of nickel nanoparticle ceramic composites under percolation threshold was also found to be larger than that predicted by the percolation theory because the extremely small particle size causes tunneling effects of next nearest neighboring particles [Abdurakhmanov et al (2006)]. Therefore, simulations that can take account of these size or interface induced effects are highly desirable for accurately determining the transport properties (thermal and electrical conductivity) for random composites made of materials with high contrast ratio properties.

Most previous studies on random composites made of materials with high thermal conductivity contrast ratio were focused on *bulk* composite materials. The study of Ganapathy et al [Ganapathy et al (2005)] showed that the effective medium theory based on diffusive heat conduction can not be used to model thermal conductivity of composites with high volumetric concentration of the

conductive materials because the percolation effects are not taken accounted for. Thovert et al [Thovert et al (1990)] solved the Laplace equation in the two- and three- dimensional random insulator-conductor composites (porous media) and the conductivity exponents of the composites are found to be close to those of percolation network. Liang and Ji [Liang and Ji (2000)] numerically studied thermal conductivity of random composites and found that the percolation threshold of thermal conductivity for three dimensional composites is around 0.4. Gerenrot et al [Gerenrot et al (2003)] performed a random network analysis for the composite materials and found that the thermal conductivity beyond the percolation threshold is almost linear with volumetric concentration. These studies mostly focused on how geometry may affect thermal transport and the interface thermal resistance was neglected. The effects of thermal interface resistance on the thermal conductivity percolation in composites were examined by Devpura et al [Devpura et al (2001)].

Recent modeling efforts on thermal transport in random nanocomposites are mostly inspired by the experimental demonstration of significant improvements of thermal conductivity in polymer - carbon nanotube composites [Biercuk et al (2002)]. Nan et al [Nan et al (2004)] used a simple effective media approach to explain the thermal conductivity enhancement in the polymer-carbon nanotube composites. Kumar et al [Kumar et al (2007)] recently studied the role of nanotube percolation on the effective thermal conductivity of the polymer nanocomposites using a finite volume model. Foygel et al [Foygel et al (2005)] developed a Monte Carlo code to randomly disperse carbon nanotube in a composite and showed that geometrically the percolation threshold is extremely low due to the high aspect ratio of the nanotubes. Shenogina et al [Shenogina et al (2005)] simulated the thermal transport between different nanotubes and explained the lack of the thermal percolation in polymer matrix- carbon nanotube composites due to the limited heat transfer rate at the small contact areas between the nanotubes. Duong et al [Duong et al (2005)] performed random walk simulations for thermal transport in carbon nanotube-polymer composites with up to 8% of nanotube fillers and found that the thermal conductivity was smaller than the prediction by Maxwell theory due to significant interface thermal resistance. No percolation phenomena were reported in their study. However, carbon nanotubes typically have very high aspect ratio and occupy a small volumetric concentration of the composites in these studies, the results therefore may not be able to extrapolate to composites with a wider range of volumetric concentrations. More importantly, the thermal transport in the composites was either modeled by the Fourier's law [Nan et al (2004), Kumar et al (2007), Shenogina et al (2005)] or a simplified random walk model [Duong et al (2005)]. It is known that thermal transport in nanocomposites is a ballistic-diffusive transport process which cannot be simply captured by Fourier heat conduction theory and the added thermal interfacial resistance [Yang and Chen (2004), Chen (1998)]. Therefore, previous models for predicting composite thermal conductivity based on solving the heat diffusion equation may lack the predictive power for the thermal conductivity of nanocomposites. A valuable tool to study the thermal transport in crystalline nanocomposites is the phonon Boltzmann transport equation when the characteristic size of the nanoparticles and nanowires is less than phonon mean free path. The solution of the phonon Boltzmann transport equation can be obtained by deterministic methods similar to those employed in radiative heat transfer or Monte Carlo simulations. However, previous studies mostly focused on simple geometries such as thin films [Chen (1998), Majumdar (1993), Mazumder and Majumdar (2001), Lacorix et al (2005)], or unit cells with limited number of nanoparticles [Yang and Chen (2004), Yang et al (2005) Jeng et al (2008)]. These models therefore can not be used for modeling the percolation phenomena that occur in composites containing a large number of particles. Although the general principles of the Monte Carlo method [Jeng et al (2008), Mazumder and Majumdar (2001), Lacroix et al (2005)] can be applied for any geometric complexity, modifications or simplifications are needed to render the simulations feasible

for random composite simulation domain containing hundreds or more particles with high thermal conductivity contrast ratio.

In short, there is an immediate need to obtain the thermal conductivity of random nanocomposites in bulk form for various applications and to understand how the phonon-interface scattering might affect the thermal conductivity of random nanocomposites. For the random and geometric percolation scenario, previous periodic unit cell approach with limited number of nanowires or nanoparticles in the composites [Yang and Chen (2004), Yang et al (2005), Jeng et al (2008)] can not be used to predict the transport properties. The aims of this study are therefore set forth: (1) to extend the Monte Carlo simulation of phonon transport for thermal conductivity prediction in three-dimensional randomly distributed nanoparticle composites, especially when the constituents are with high thermal conductivity contrast ratio; (2) to examine the effects of important factors including phonon-interface scattering, nanoparticle size, and intrinsic thermal conductivity contrast ratio on the effective thermal conductivity of the nanoparticle composites.

2 Numerical Simulation Procedure

The effective thermal conductivity of the random composites is obtained by modeling phonon transport using the Monte Carlo method in a simulation domain that contains a large number of randomly distributed nanoparticles. We describe in detail in this section the generation of random distribution of nanoparticles in the simulation domain, a modified drifting-scattering scheme [Jeng et al (2008), Mazumder and Majumdar (2001)] that is based on our previous work but with significantly reduced computation cost, and relevant physics behind the simulation.

2.1 Generation of Random Composites and Simulation Domains

The composites considered in this study are made of nanoparticles of two different materials randomly distributed in the simulation domain. The periodic unit cell approach with limited number of nanowires or particles [Yang and Chen (2004), Jeng et al (2008)] employed in previous studies can not be applied to the current nanocomposites because of the random distribution and geometric percolation of the nanoparticles. Instead, we applied the "representative volume element" (RVE) [Drugan and Willis (1996), Kanit et al (2003), Ren and Zheng (2002), Okada et al (2004), Wang and Yao (2005)] containing many nanoparticles, to obtain the effective thermal conductivity. The RVE concept has been widely used for modeling mechanical and thermal properties of macroscopically homogeneous but microscopically heterogeneous composite material. In our case, the RVE can be regarded as the volume contains a sufficiently large number of nanoparticles so that the volume is a statistically representative of the random composites simulated, i.e. the thermal conductivity of the RVE represents that of the random composites. The minimum number of nanoparticles required in the RVE is numerically determined as discussed in section 3.1. A schematic of the composites considered in this study is shown in Fig. 1. The nanoparticles are assumed to be cubical in this study. Geometrically the RVE is made of $N_t = N_x \times N_y \times N_z$ number of equal sized cubical nanoparticles, where N_t is the total number of nanoparticles in the RVE, N_x, N_y and $N_z$is the number of nanoparticles in x, y and z coordinates, respectively.

The random arrangement of the nanoparticles is realized by generating three random numbers that determine the x, y and z coordinates for each nanoparticle of one material in the RVE. Firstly, the simulation domain is uniformly divided into $N_t = N_x \times N_y \times N_z$ lattice sites, with each nanoparticle occupying one lattice site. To improve the numerical resolution of the simulation results, each nanoparticle is further divided into a number of sub-elements. These sub-elements allow the temperature gradients to develop within the particles, so that the thermal resistance of the particles can be taken into account, especially for the particles with low thermal conductivity. The positions (indices) of a nanoparticle are then determined by

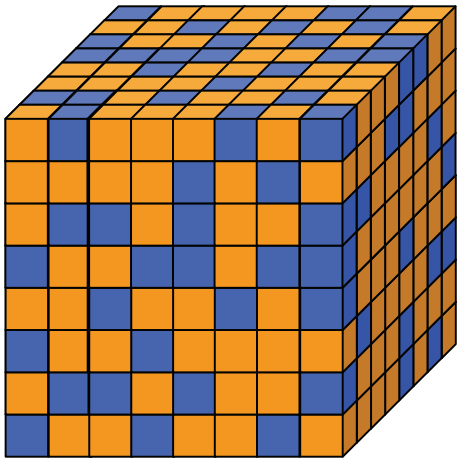

Figure 1: Schematic of nanoparticle composites. The composite materials compose of uniform sized cubic nanoparticles of two different materials randomly dispersed in space. Beyond the geometric percolation threshold, nanoparticles made of the same material can form a large cluster that connects one boundary to the opposite.

the following equations:

$$\begin{aligned} i &= INT(R_x \times N_x) \\ j &= INT(R_y \times N_y) \\ k &= INT(R_z \times N_z) \end{aligned} \tag{1}$$

where i, j and k is the indices of the nanoparticle in x, y, z coordinates, respectively, *INT* is a function to find the nearest integer, and R_x, R_y and R_z are three random numbers uniformly distributed in (0,1). In this study, a pseudo-random number generator RANLUX [Lüscher (1994)] is employed for all random number generations. This arrangement process is done in sequence. If a nanoparticle overlaps a site that has already been occupied by an existing nanoparticle, three new random numbers are generated to find a new site for the nanoparticle. This process is repeated until an empty site is found for the nanoparticle. After filling all the nanoparticles of one material randomly, the rest of the sites in the RVE are then filled with nanoparticles of the other material. This way, the randomness of the nanoparticle is ensured with the statistical randomness of the random number generators. The number of the nanoparticles of one material versus the other is determined by their volumetric concentrations, $N_i = INT(\Phi_i N_t)$, where N_i and Φ_i is the number and volumetric concentration of nanoparticles of one material in the composites. Therefore, the exact volume concentration of different materials can be satisfied within the error of half of nanoparticle, corresponding to a relative error less than $1/2N_t$ in the composites. Other schemes to generate the random distribution of the nanoparticles are also possible. For example, one can determine each individual lattice site occupied with which material by comparing a random number with its volumetric concentration. However, this scheme can not guarantee the exact volumetric concentration due to the statistical fluctuation of the random numbers and was not adopted in this study. Finally, the interfaces between the same type of nanoparticles are removed, so that the same type of nanoparticles with common faces are continuous and form clusters. The numerical cluster forming process represents the physical recrystallization [Mayrhofer et al (2003)] or melting processes after the nanoparticles are mixed to fabricate nanocomposites The faces for different types of nanoparticles form the interfaces for the phonon scattering.

2.2 Phonon Properties and Transport

For most semiconductor and dielectric materials, phonons (quantized lattice vibrations) are the main energy carriers for heat conduction [Kittel (1986), Chen (2005)]. This work is built upon previous studies on the phonon transport in nanoscale structures using Monte Carlo simulations. We would like to note that the framework of this paper assumes that phonon concept is still valid in nanocomposites. This is generally true as long as the nanocomposites form crystalline structures. Though the phonon spectrum in nanostructures can be different from bulk materials, our simulation uses bulk phonon dispersion for constituent materials. This is due to the two reasons [Chen (1998)]: (1) the change of phonon spectrum, such as density of state and the group velocity of phonons in nanostructures, is not the most significant reason for thermal conductivity reduction in nanostructures; (2) recent experi-

ence with superlattices suggests that the idealized phonon dispersion in nanostructures is difficult to realize experimentally, because it is difficult to obtain sufficiently smooth and uniform surfaces for coherent interference. In other words, the interface of nanocomposites often induces diffuse scattering which makes the formation of phonon minibands rather difficult. The phonon transport therefore follows the Boltzmann transport equation:

$$\frac{\partial f}{\partial t} + \mathbf{v} \bullet \nabla_{\mathbf{r}} f = \left(\frac{\partial f}{\partial t} \right)_c \tag{2}$$

where f is the phonon distribution function, t is time, v is the phonon group velocity vector, r is the position vector, and the right hand side of the equation represents the phonon scattering term. Monte Carlo simulation that tracks the drifting and scattering of phonon energy bundles is used to model phonon transport governed by the Boltzmann transport equation. Although phonon spectral properties can be accounted for in Monte Carlo simulation, a phonon gray media approximation [Yang and Chen (2004), Yang et al (2005), Jeng et al (2008), Chen (1998)] is employed in this study where the average phonon properties at equilibrium state are assigned to the phonon energy bundles. The average frequency and group velocity of the phonon bundles are estimated by averaging the equilibrium phonon dispersion curve of three branches of acoustic phonons in silicon [Brockhouse (1959)]. The mean free path for phonon transport is estimated by the kinetic theory and experimental intrinsic thermal conductivity. Similar approximations have been employed in previous studies for phonon transport in superlattices [Chen (1998)] and nanocomposites [Jeng et al (2008)] in which the simulation results agree well with experimental data. In the parametric study, we vary the intrinsic thermal conductivity by adjusting the phonon mean free path, as discussed in section 3.1.

The average frequency of the phonons at a temperature can be calculated as:

$$\omega_{avg} = \frac{1}{N} \sum_{p=1}^{3} \int_0^{\varpi_{mp}} \omega \langle n \rangle D(\omega) \, d\omega \tag{3}$$

where p is the polarization branch index, ω_{mp} is the maximum cutoff frequency of each phonon branch, ω is the phonon frequency and $\langle n \rangle$ is the Bose-Einstein distribution. $D(\omega)$ is the phonon density of state for each branch,

$$D(\omega) = \frac{k^2}{2\pi^2} \frac{\partial k}{\partial \omega} \tag{4}$$

in which k is the magnitude of the phonon wave vector. N is the phonon number density,

$$N = \sum_{p=1}^{3} \int_0^{\omega_{mp}} \langle n \rangle D(\omega) \, d\omega \tag{5}$$

The average group velocity of the phonon energy bundle can be calculated as:

$$v_{avg} = \frac{1}{N} \sum_{p=1}^{3} \int_0^{\omega_{mp}} \frac{\partial \omega}{\partial k} \langle n \rangle D(\omega) \, d\omega \tag{6}$$

The mean free path for phonon transport is calculated based on the kinetic theory,

$$\Lambda = \frac{3 k_{bulk}}{v_{avg} C_{ac}} \tag{7}$$

where k_{bulk} is the thermal conductivity of the bulk media, which can be obtained from experimental data in the literature. In the above calculations, we assume that three branches of acoustic phonons contribute primarily to the thermal conductivity of the material and the contribution of the optical phonons is insignificant due to their small group velocity [Chen (1998)]. C_{ac} is the heat capacity of the acoustic phonons:

$$C_{ac} = \sum_{p=1}^{3} \int_0^{\omega_{mp}} \hbar \omega \frac{\partial \langle n \rangle}{\partial T} D(\omega) \, d\omega \tag{8}$$

In the Monte Carlo simulation, phonon energy bundles with the above calculated average frequency and group velocity are initialized and allowed to drift in the RVE. A prescribed heat flux to generate the temperature gradients for thermal conductivity calculation is then applied at the boundaries perpendicular to the x coordinates by emitting appropriate number of phonon bundles at these boundaries. These phonon energy bundles

also encounter different scattering events, which create thermal resistance in the nanoparticle composites. The thermal conductivity of composites is calculated after the temperature field in the RVE reaches the steady state condition. The following sections provide a detailed description of the Monte Carlo simulation procedure of phonon transport.

2.3 Phonon Initialization and Drift

The initial condition of the RVE is set to be in equilibrium. Due to the statistical nature of the Monte Carlo method, the noise to signal ratio is determined by the number of phonon bundles simulated. The more phonon bundles tracked in the Monte Carlo simulation, the higher accuracy of the simulation results. However, to track a large number of phonon bundles requires large memory and long computational time. Therefore, the number of phonon bundle simulated is based on a balance choice of computational time and accuracy requirement. Since the number of simulated phonon energy bundles is much smaller than the actual phonon numbers in the materials [Mazumder and Majumdar (2001), Lacorix et al (2005)], a scaling factor, for which each simulated phonon bundle represents S actual phonons, is needed:

$$S = \frac{N_a}{N_s} = \frac{C_{ac} T V / \hbar \omega_{avg}}{N_s} \tag{9}$$

where N_a and N_s represent the number of actual phonons and simulated phonons in a sub-element, T and V are the temperature and volume of the sub-element. Equation (9) can also be used to calculate the temperature of the sub-element in the subsequent simulation procedure. Due to equilibrium, the phonon bundles in each material are uniformly distributed in space. The directions of phonon bundles are randomly oriented in the computational domain. The direction vector is given by:

$$\hat{s} = \hat{i}\cos\theta + \hat{j}\sin\theta\cos\phi + \hat{k}\sin\theta\sin\phi \tag{10}$$

where the polar angle is determined by $\cos\theta = 2R_1 - 1$ and the azimuthal angle is determined by $\phi = 2\pi R_2$. R_1 and R_2 are two independent random numbers uniformly distributed between (0,1).

At each time step, phonon bundles are allowed to drift with group velocity. The positions (spatial coordinates) of phonon bundles at a new time step are calculated as:

$$x_N = x_O + v_{avg}\Delta t\cos\theta \tag{11}$$

$$y_N = y_O + v_{avg}\Delta t\sin\theta\cos\phi \tag{12}$$

$$z_N = z_O + v_{avg}\Delta t\sin\theta\sin\phi \tag{13}$$

where subscript "$_N$" and "$_O$" denotes phonon coordinates at new and old time step. To achieve the necessary grid resolution, the time step Δt is chosen that the phonon bundles are drifted less than a sub-element within a time step.

2.4 Phonon Scattering

The thermal resistance of nanocomposites is caused by two categories of phonon scattering mechanism: intrinsic scattering including phonon-phonon, phonon-impurities, phonon-dislocation scattering and phonon scattering at interfaces between different materials. A modified drift-scattering scheme is employed in this study for phonon intrinsic scattering. The phonon interface scattering is assumed to be partially diffusive and partially specular in the Monte Carlo simulation. The implementation of these scattering processes is presented in the rest of the section.

Intrinsic scattering is the main mechanism creating thermal resistance in bulk materials. The details of these scattering are not well understood and modeling them in Monte Carlo simulation is time consuming and difficult to obtain high accuracy[Mazumder and Majumdar (2001), Lacorix et al (2005)], a lumped mean free path approximation [Jeng et al (2008)] is instead used in this study. In this approximation, the probability of a phonon scattering is written as:

$$P_s = 1 - \exp(-v_{avg}\Delta t/\Lambda) \tag{14}$$

Similar to previous Monte Carlo simulations for phonon transport [Mazumder and Majumdar (2001), Jeng et al (2008)], the intrinsic scattering is performed at the end of each time step for the phonon drift phase. A random number is generated for every phonon bundle. If $R_i < P_s$, the

phonon bundle undergoes an intrinsic scattering event. The scattering is assumed to be isotropic, where the direction vector of the phonon bundle after scattering is reset to be randomly distributed over a solid angle, similar to the process in the phonon initialization.

There is no explicit limitation for the above scattering probability calculation in the Monte Carlo simulation. In practice, however, when $v_{avg}\Delta t \ll \Lambda$ or the phonon mean free path is much larger than the drifting distance, the scattering probability become extremely small ($P_s \to 0$) and a large number of phonons are needed to sample the scattering probability accurately and the Monte Carlo simulation becomes inefficient. On the other hand, when the drifting distance is much larger than the phonon mean free path, the scattering probability approaches to one and almost all phonons get scattered after drifting. The phonon drifting directions in the domain become isotropic, and the temperature gradients can take long time to establish in the Monte Carlo simulation. Indeed, the current drift-scattering scheme is not valid when the drifting distance is longer than the phonon mean free path, because the scattering is performed after the phonon drifting phase, which indicates that no scattering occurs within the drifting distance. Therefore, every phonon is allowed to drift longer distance than the mean free path, which is in conflict with the definition of the phonon mean free path and the Monte Carlo simulation will over-predict the thermal conductivity. Several remedies are possible, for example, one can further divide the drifting distance into a number of smaller distances so that each of them is smaller than the phonon mean free path. Or one can calculate the scattering free distance: $d = -\Lambda \ln(1 - R_i)$ and compare it with the drifting distance $v_{avg}\Delta t$. In either case, multi-scattering events are possible within one time step and due to the interface scattering described in the next paragraph, the process flow of the Monte Carlo code becomes complicated and less efficient. In the current simulations, we adopted a strategy to ensure that the drifting distances of the phonons energy bundles smaller than the phonon mean free paths of both materials in the composites. The noise caused by $v_{avg}\Delta t \ll \Lambda$ in one phase of material is less problematic because the significant interface scattering in the nanoparticle composites, as described in the next paragraph.

Phonon-Interface scattering caused by a phonon intersecting interfaces between different materials is an important phonon scattering mechanism that creates thermal resistance in nanoparticle composites. Existing theories such as modeling phonon interface scattering as acoustic waves [Chen (1999)] across interfaces generally involve many assumptions and are cumbersome to implement in the Monte Carlo simulation. In addition, the interfaces properties may be affected by different modifications [S. Namilae et al (2007)]. Therefore, we simplified the interface scattering modeling based on several characteristics such as the roughness of the interface. Phonons are diffusively scattered with no preferential directions when the roughness of the interface is much larger than phonon wavelength, while scattering are specular when the interface is smooth compared with the phonon wavelength [Chen (2005)]. We define the specularity, S_p, as the ratio of specular scattering events and total scattering events at the interface with $S_p = 0$ for completely diffusive interface scattering and $S_p = 1$ for completely specular scattering, to account for the partially specular, partially diffusive scattering at the interface. A random number R_s is generated for each scattering event to take account for the specularity of the interfaces. If $R_s < S_p$, the phonon interface scattering is specular and undergoes specular reflection and transmission. Otherwise, the phonon scattering is diffusive. The phonon drifting direction after specular reflection is model as:

$$\mathbf{s}_r = \mathbf{s}_i - 2(\mathbf{s}_i \bullet \hat{n})\hat{n} \tag{15}$$

where $\mathbf{s}_r$ and $\mathbf{s}_i$ represent the reflected and incident phonon direction vectors, respectively. $\hat{n}$ is a unit vector normal to the interface. In specular transmission, we assume phonons do not change drifting directions across the interface. The direction of a phonon after diffusive transmission or reflection is modeled according to the interface normal

and tangent vectors:

$$\mathbf{s} = \pm\hat{n}\cos\theta' + \hat{t}_1 \sin\theta'\cos\phi' + \hat{t}_2 \sin\theta'\sin\phi' \tag{16}$$

The polar angle θ' and azimuthal angle ϕ' in Eq. (16) can be determined by $\theta' = \sin^{-1}\left(\sqrt{R_3}\right)$ and $\phi' = 2\pi R_4$, where R_3 and R_4 are two random numbers. Note that the angles are with local interface, therefore, a transformation of θ' and ϕ' to global θ and ϕ is needed to track the phonon according to the global coordinates.

The phonon transmissivity and reflectivity at the interface is estimated by:

$$T_{12} = \frac{CU_2v_2}{U_1v_1 + U_2v_2} \tag{17}$$

$$R_{12} = 1 - T_{12} \tag{18}$$

where T_{12} and R_{12} is the phonon transmissivity and reflectivity from medium 1 to 2, C is an adjustable constant and Eq. (17) agrees with the diffusive mismatch model [Dames and Chen (2004)] previously derived when $C = 1$, U is the phonon energy density. C is chosen to be unity for most cases in this study, except when the effects of phonon interface tramsmissivity are investigated in section 3.4. It can be shown that Eq. (17) and (18) satisfy the detailed energy balance across interface at thermal equilibrium, i.e. there is no net heat flux across interface when material are at thermal equilibrium. A random number R_t is generated to compare with the transmissivity of the interface T_{12}. If $R_t < T_{12}$, the phonon is transmitted through the interface. Otherwise, the phonon is reflected at the interface.

The interface scattering occurs when the phonon path within a time step from (x_O, y_O, z_O) to (x_N, y_N, z_N) has intersection with the interfaces. In previous models [Tian and Yang (2007a)], the positions of the interfaces were pre-stored in computer memory after setting up the simulation domain. Then a global searching is performed to find the appropriate intersection (x'_N, y'_N, z'_N), which needs to lie within the phonon path and the interface. Mathematically, (x'_N, y'_N, z'_N) is the solution that satisfies both equations for the line describing the phonon path and the plane describing the interface. However, this global searching algorithm becomes vastly inefficient and becomes a bottleneck for computational time as the number of interfaces dramatically increases with the number of particles in the composites. In each time step, the number of searches needed is on the order of $\frac{1}{2}N_iN_a$, where N_i is the number of interfaces in the simulation domain. The current simulation employs an improved algorithm that only checks the interfaces of the nearest and next nearest neighboring sub-elements from the sub-element (x_O, y_O, z_O) is located. It was estimated that the number of interface searches for each time step decreases to $\frac{1}{2} \times 54 \times N_a$, where 54 represents the number of possible scenarios of a phonon path intersecting with an interface in this study. To further increase the computational efficiency, a number of other improvments is employed. For example, if both (x_O, y_O, z_O) and (x_N, y_N, z_N) locate within the same sub-element or nanoparticle, no interface scattering search is needed. When the phonon energy bundle is located close to the edge or corner of the nanoparticle, multiple scattering events may occur. After the first scattering, (x_O, y_O, z_O) is replaced by the intersection (x'_N, y'_N, z'_N) for the next intersection search. However, the phonon bundle is located on the interface and the solution which is the starting position of the phonon bundles needs to be eliminated. We can achieve this elimination by rejecting intersection solution within a certain distance from the starting position. The multiple interface searches are performed until the accumulated time for phonon drifting between multiple scattering events approaches the total time step.

Phonon bundles after intrinsic scattering or interface scattering have different frequencies and the energy conservation is not observed. Previous Monte Carlo simulations employed different phonon creation-destruction schemes [Jeng et al (2008), Mazumder and Majumdar (2001)] or an adjusted phonon distribution function [Lacroix et al (2005)] to ensure the energy conservation. In the current simulation, no frequency re-sampling is performed after phonon intrinsic scattering because of the phonon gray media approximation and assuming the material properties independent

of temperature change, which implies that the thermodynamic temperature of the simulation domain does not deviate significantly from the initial equilibrium temperature. For phonon bundles cross the interface between two materials, the actual phonon frequency changes if the materials have different average phonon frequencies ω_{avg}. However, the energy conservation can be achieved by adjusting the scaling factor for each material in the initial condition so that each simulated phonon energy bundles in both materials have the same amount of energy albeit different frequencies, i.e. the phonon creation-destruction in interface scattering is incorporated in the scaling factor and no explicit creation-destruction scheme [Jeng et al (2008), Mazumder and Majumdar (2001)] is used.

2.5 Boundary Conditions

The RVE is assumed to be periodically stacked to form the nanoparticle composites. The periodic boundary conditions can be applied to simulate the phonon transport in the RVE due to the geometric periodicity. This is valid when the RVE is located far away from the surface of the bulk nanocomposites. However, there are interfaces at the boundaries between the periodically stacked RVEs and interface scattering poses a problem for implementing such periodic boundary conditions, because the diffusive phonons scattering from the interface change drift directions and destroy the periodicity. To overcome this problem, the simulation domain is shifted from the original RVE described in section 2.1 by half of a nanoparticle size in all x, y, z coordinates so that the boundaries of the simulation domain do not contain interfaces. A similar procedure for two dimensional nanowire composites was performed in our previous study [Tian and Yang (2007b)] where more details were given. The boundary conditions at y = 0 and y = Ly (Ly is the size of the simulation domain in y coordinate) are set to be periodic, i.e. for each phonon leaving a boundary, a phonon with exactly the same direction, position and velocity enters from the opposite boundary. Similarly, the boundary condition at z = 0 and z = Lz (Lz is the size of the simulation domain in z coordinate) are also assumed to be periodic. For boundaries at x = 0 and x = Lx (Lx is the size of the simulation domain in x coordinate), a specified heat flux is applied to generate the temperature gradients needed to obtain thermal conductivity,

$$\mathbf{q}(y,z)|_{x=0} = \mathbf{q}(y,z)|_{x=L_x} \tag{19}$$

where q is the heat flux. To ensure the identical heat flow distribution along the two boundaries, the pattern of phonons emitted at one boundary is the same as the pattern of phonons leaving the opposite boundaries. The effective thermal conductivity k_{eff} of the simulation domain is then obtained by:

$$k_{eff} = \frac{\overline{q}}{\Delta\overline{T}} L_x \tag{20}$$

where

$$\overline{q} = \frac{1}{L_z L_y} \int_0^{L_z} \int_0^{L_y} q|_{x=0} \, dydz \tag{21}$$

$$\Delta\overline{T} = \frac{1}{L_z L_y} \int_0^{L_z} \int_0^{L_y} \left(T|_{x=0} - T|_{x=L_x} \right) dydz \tag{22}$$

3 Results and Discussion

3.1 Model Validation

The developed Monte Carlo phonon transport code was extensively tested before it is used for three dimensional random nanoparticle composites. We compared the predicted temperature-dependent thermal conductivity for bulk Si with experimental data and found good agreements. The predictions of the current Monte Carlo code for the thermal conductivity of two- and three- dimensional periodic nanocomposites were found to agree well with previously reported results [Yang and Chen (2004), Jeng et al (2008)]. Figure 2 shows one of the comparisons of thermal conductivity for two dimensional periodic Si-Ge nanowire composites calculated by the deterministic solution [Yang and Chen (2004)] and the current Monte Carlo code. The thermal conductivity

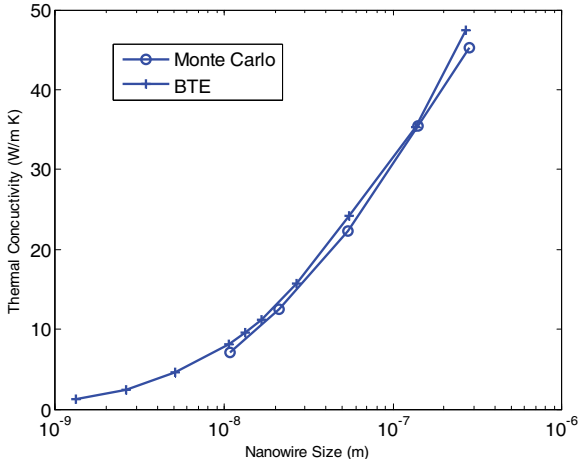

Figure 2: Comparison of thermal conductivity of two dimensional periodic Si-Ge nanowire composites predicted by solving the phonon Boltzmann transport equation (BTE) using deterministic solution [Yang and Chen (2004)] (denoted as BTE in the figure) and the Monte Carlo simulation.

obtained by both methods agrees well with each other for different nanowire size.

Before examining the phonon transport and thermal conductivity percolation in the nanoparticle composites, one important question needs to be answered is how many nanoparticles the RVE should contain so that the thermal conductivity of the RVE represents that of the composites. Two numerical approaches can be taken to verify whether the number of nanoparticle is large enough. The first approach is to compare the thermal conductivity of RVEs with different independent random distributions of nanoparticles. The number of nanoparticle would be large enough if the thermal conductivity does not deviate from each other significantly. This can be achieved by using different seeds in initializing the random number generator to distribute the nanoparticles as described in section 2.1. An additional approach is to compare the thermal conductivity of RVEs with different number of nanoparticles and if the thermal conductivity does not vary significantly, the number of nanoparticles is sufficient. Both approaches were employed in this study. The results of the latter approach were shown in Fig. 3. The nondimensionalized effective thermal conductivity is defined by k_{eff}/k_2, where k_{eff} is the effective thermal conductivity of the nanoparticle composites. The horizontal axis is the volumetric concentration, Φ_1, of the high thermal conductivity constituents. The intrinsic thermal conductivity contrast ratio k_1/k_2 is 100, where subscript 1, 2 denote the high and low thermal conductivity constituents, respectively. In this study, the thermal conductivity difference of the constituents is generated by multiplying the silicon phonon mean free path obtained from Eq. (7) with different values while keeping the group velocity and specific heat constant. Based on the simple kinetic theory, the contrast ratio of the intrinsic thermal conductivity equals to that of the phonon mean free path, or $k_1/k_2 = \Lambda_1/\Lambda_2$. The nanoparticle size is 30 nm. Figure 3 also presents a comparison of thermal conductivity for simulations with each nanoparticle containing $8(2\times2\times2)$ and $64(4\times4\times4)$ cubical sub-elements. In the simulation results, we found the difference of thermal conductivity for the RVEs containing 1000 $(10\times10\times10)$ and 2197 $(13\times13\times13)$ nanoparticles is within 6% for all volumetric concentrations. In addition, no significant improvement was found when the number of sub-elements in the nanoparticle increase from 8 to 64. Therefore, all the results presented in this paper were carried out with 1000 nanoparticles in the RVE and each particle containing 8 cubical sub-elements.

3.2 Effect of Nanoparticle Size

The nanocomposite thermal conductivity is very sensitive with the nanoparticle size, especially when the phonon transport in the composites is ballistic [Yang and Chen (2004)]. Figure 4 shows the size dependence of the nondimensionalized effective thermal conductivity for random nanoparticle composites. The thermal conductivity contrast ratio $k_1/k_2 = \Lambda_1/\Lambda_2$ is assumed to be 100. The nanoparticle sizes, denoted as a in the figure, are 6 nm, 30 nm and 150 nm, with Λ_2/a approximately equals to 5, 1, and 1/5, respectively. The dashed line represents the effective thermal conductivity k_{eff} beyond percolation threshold predicted by a revised scaling law [Ma-

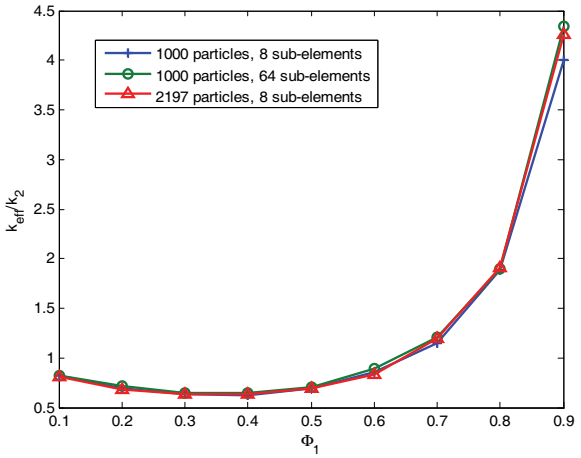

Figure 3: Thermal conductivity predictions for the RVE containing 1000 and 2197 nanoparticles and each nanoparticle containing 8 and 64 cubical sub-elements. The good agreement between results of a RVE containing 2197 and 1000 nanoparticles, 8 sub-elements shows that the thermal conductivity of a RVE with 1000 nanoparticle statistically represents that of the nanoparticle composites. The agreement between results of a RVE 1000 nanoparticle with each nanoparticle containing 8 and 64 sub-elements demonstrates that further refinement of mesh is not necessary. All the subsequent simulations are therefore based on a RVE containing 1000 nanoparticles and each nanoparticle divided into 8 cubical sub-elements.

munya et al (2002)]:

$$\frac{k_{eff}-k_2}{k_1-k_2}=\left(\frac{\Phi_1-\Phi_c}{1-\Phi_c}\right)^2 \tag{23}$$

where Φ_c is the percolation threshold and the conductivity exponent $t=2$. Equation (23) agrees both the scaling law predicted by the percolation theory and the physical bound of the thermal conductivity, i.e. when $\Phi_1=1$, $k_{eff}=k_1$. The nondimensionalized effective thermal conductivity of all volumetric concentration decreases with decreasing nanoparticle size because of increasing interface density, defined by the interfacial area per unit volume. When the size of the nanoparticle is larger than the mean free path of the lower thermal conductivity material ($\Lambda_2/a=1/5$), the effective thermal conductivity increases monotonically with the volumetric concentration of the high thermal conductivity material. However, the rate of change for the thermal conductivity of the nanoparticle composites is much smaller than predicted by Eq. (23), even when the volumetric concentration of the high thermal conductivity constituents is larger than 0.3116, which is the percolation threshold for the cubic lattices [Stauffer and Aharony (1991)] This is because the percolating channels that connect the opposite boundaries of the composites are torturous and the effective width of the channels are not much larger than the nanoparticle size, which is smaller than the phonon mean free path of the high thermal conductivity constituents. Therefore, interface scattering dominates the thermal resistance and the percolating network is not effective in promoting phonon energy transport. For comparison, the effective thermal conductivity of the three dimensional bulk composites with the same thermal conductivity contrast ratio of the constituents [Liang and Ji (2000)] is also plotted in the figure. The thermal conductivity of the bulk composites is higher than that predicted by Eq. (23), although they agree with each other at high Φ_1. In fact, the thermal conductivity of nanoparticle composites with $\Lambda_2/a=1/5$ is also larger than that predicted by Eq. (23) for a small range of Φ_1 close to Φ_c. This is probably because conventional percolation theory does not take account of the transport within the low thermal conductivity constituents in the composite [Stauffer and Aharony (1991)]. However, for the composites made from particles with thermal conductivity contrast ratio of 100, the thermal transport in the low conductivity constituent is accounted for, thus yields higher thermal conductivity. The effect of thermal conductivity contrast ratio of the constituents on the effective thermal conductivity of the nanoparticle composites is discussed in the next section.

When the nanoparticle size is further decreased to 30 nm and 6 nm, or $\Lambda_2/a=1$ and 5, phonon transport in both materials is ballistic and the thermal conductivity in the nanoparticle composites actually decreases with increasing high thermal conductivity volumetric concentration even beyond percolation threshold. This phenomenon was not observed in previous studies for bulk composites

even when the thermal interface resistance between the two materials is very high [Devpura et al (2001)]. However, such a reduction of thermal conductivity due to increase of interface density was observed in models for SiGe nanocomposites [Yang et al (2005)] and in experiments for Si3N4/SiC nanocomposites [Hirano et al (1995)]. This is due to the dominance of interface scattering in phonon ballistic transport regime. Due to geometric symmetry, the maximum interface density occurs at $\Phi_1 = \Phi_2 = 0.5$. Therefore, the magnitude of the effective thermal conductivity is determined by the competition between the increase of the interface density which lowers the thermal conductivity, and the increase of volumetric concentration of high thermal conductivity constituents which improves the thermal conductivity. The minimum thermal conductivity of the nanocomposites therefore occurs at Φ_1 slightly smaller than 0.5.

3.3 *Effect of Thermal Conductivity Contrast Ratio*

One of the techniques to improve the effective thermal conductivity of composite material is to disperse high thermal conductivity material such as metallic, carbon nanotube or graphene fillers into the low thermal conductivity matrix such as polymers. The extremely high thermal conductivity of carbon nanotubes recently observed [Hone et al (1999), Berber et al (2000), Kim et al (2001), Pop et al (2006)] attracted many excitements for such applications [Biercuk et al (2002)]. Previous modeling studies on random composites all showed a significant impact of the material contrast on the effective properties of the composites [Ganapathy et al (2005), Liang and Ji (2000), Devpura et al (2001)]. In this section, we investigated the effect of the intrinsic thermal conductivity contrast ratio defined as $k_1/k_2 = \Lambda_1/\Lambda_2$ between the constituent materials on the effective thermal conductivity of the nanoparticle composites.

Figure 5 shows that the thermal conductivity contrast ratio plays a limited role in determining the nondimensionalized effective thermal conductivity (k_{eff}/k_2) of the nanoparticle composites when

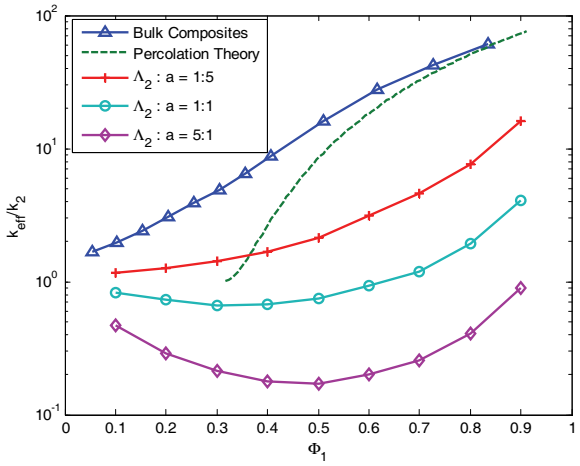

Figure 4: Effect of the nanoparticle size on the nondimensionalized effective thermal conductivity of nanoparticle composites. The thermal conductivity contrast $k_1 : k_2 = \Lambda_1 : \Lambda_2$ between the nanoparticles is assumed to be 100. The thermal conductivity of nanocomposites made of the smallest nanoparticle continue to decreases with increasing high thermal conductivity constituents volumetric concentration beyond its percolation threshold of 0.3116, which demonstrates that the interface density dominates the phonon transport and percolating network is not effective in improving thermal conductivity when phonon transport is ballistic. The dashed line is calculated according to equation (23).

the nanoparticle size, a, is similar to the phonon mean free path of the low thermal conductivity constituents, Λ_2. For $\Lambda_1 : \Lambda_2 : a = 10 : 1 : 1$ and $\Lambda_1 : \Lambda_2 : a = 100 : 1 : 1$, the nondimensionalized effective thermal conductivity k_{eff}/k_2 moderately increases at very high volumetric concentrations of the high thermal conductivity constituents Φ_1, while the difference of k_{eff}/k_2 at low Φ_1 is very small. As the contrast ratio of intrinsic thermal conductivity is further increased from $\Lambda_1 : \Lambda_2 : a = 100 : 1 : 1$ to $1000 : 1 : 1$, no further improvement of the nondimensionalized effective thermal conductivity is observed for Φ_1 from 0.1 to 0.9. This trend can be explained as the following. For composites with low volumetric concentration of high thermal conductivity constituent, percolation network can not be formed and the ther-

mal conductivity of the composites is effectively controlled by the low thermal conductivity constituents and phonon-interface scattering. Therefore, no significant difference can occur by changing the thermal conductivity of the high thermal conductivity constituents. When the volumetric concentration of high thermal conductivity consitituents is higher than the percolation threshold, geometrically percolate channels for phonon transport is formed. These channels are nevertheless torturous and the effective width of the percolating channels is not much larger than the size of the nanoparticles except at extremely high volumetric concentrations. Phonons in these percolation channels experience many interface scattering events, similar to the boundary scattering in torturous nanowires, which suppress the phonon transport. Therefore, on the contrary to the bulk composites, increasing the thermal conductivity of one type of nanoparticles only moderately increase the effective thermal conductivity initially, while further increasing the constituent thermal conductivity has negligible effect on the effective thermal conductivity of the composites. In fact, the short of high thermal conductivity contrast ratio was postulated to be the main reason for the lack of the thermal conductivity percolation in composite materials [Mamunya et al (2002)], the results of the current simulation show that improving the thermal conductivity contrast ratio of constituents is not effective in improving the phonon thermal conductivity of composites when the phonon transport in one phase of the constituent materials is ballistic.

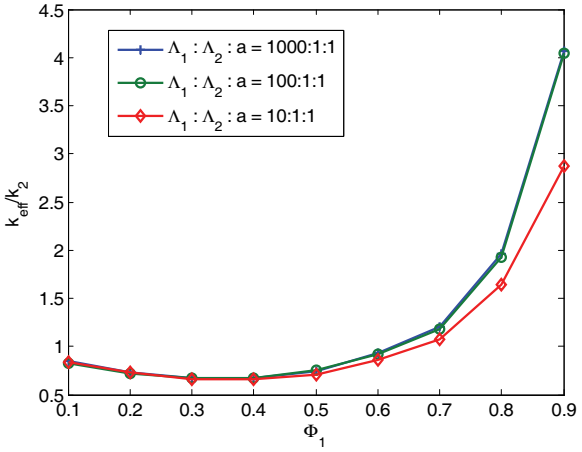

Figure 5: Effect of the constituents' intrinsic thermal conductivity contrast ratio on the nondimensionalized effective thermal conductivity of nanoparticle composites. $\Lambda_2 : a = 1 : 1$ is used in this simulation. The contrast ratio plays little role in differentiating the thermal conductivity of the composites when Φ_1 is small. At higher Φ_1, the thermal conductivity increases with increasing contrast ratio, however, further increase of the contrast ratio does not lead to higher thermal conductivity of the nanoparticle composite.

3.4 *Effect of Interface Phonon Properties*

The results of previous sections show that the phonon-interface scattering plays a critical role in determining the effective thermal conductivity of nanoparticle composites. It is thus worthwhile to investigate how the phonon-interface scattering properties may affect the thermal conductivity prediction. A more detailed study on how the phonons are reflected transmitted and converted at interfaces needs to resort to more advanced atoministic simulation tools such as molecular dynamics. For parametric study, we here vary the adjustable constant C in Eq. (17) to change the transmissivity for diffuse interface scattering with $S_p = 0$. The adjustable constant C can be regarded as a correction factor for the diffusive mismatch model [Dames and Chen (2004), Swartz, and Pohl (1989)] to account for the fact that it under-predict transmissivity for an imaginary surface within the same material [Chen (2005)] and other nanoparticle surface features such as defects, oxidization. The simulations are based on $\Lambda_1 : \Lambda_2 : a = 100 : 1 : 1$. The results are shown in Fig. 6 with transmissivity varying from $T_{12} = 0.1$ to 0.9 for concentrations of high thermal conductivity particle $\Phi_1 = 0.1$ and 0.5. The effective thermal conductivity of the composites almost linearly increases with increasing interface transmissivity. When $\Phi_1 = 0.1$, the nondimensionalized effective thermal conductivity for $T_{12} = 0.9$ is 1.3 times around larger than that for $T_{12} = 0.1$. Although not shown in Fig. 6, the nondimensionalized effective thermal conductivity for $T_{12} = 0.9$ is around 1.7 times

larger than that for $T_{12} = 0.1$ when $\Phi_1 = 0.9$. This is because the effects of interface scattering are more important when the phonon transport in the constituents is more ballistic. The effect of phonon transmissivity is also more apparent when Φ_1 is 0.5. The nondimensionalized effective thermal conductivity with $T_{12} = 0.9$ is around three times higher than that of $T_{12} = 0.1$ for $\Phi_1 = 0.5$. This is because the interface density is higher and the interface properties play a more important role in determining the thermal conductivity of composites at $\Phi_1 = 0.5$.

Figure 7 shows the effect of the specularity on the effective thermal conductivity of the nanoparticle composites. The specularity is chosen as 0, 0.5 and 1 for the cases studied where 0 corresponds to totally diffusive and 1 corresponds to totally specular scenarios. These simulations are again based on $\Lambda_1 : \Lambda_2 : a = 100 : 1 : 1$ and $T_{12} = 0.5$. The nondimensionalized effective thermal conductivity of the nanoparticle composites increases with increasing specularity for all volumetric concentration. This is because when the interface is parallel to the heat flux direction, specular reflection does not create interfacial resistance for phonon transport, while diffusive reflection does. However, specular reflection creates similar thermal resistance as diffusive reflection when the interface is perpendicular to the heat flux direction. Therefore, the thermal conductivity increase is limited by the interfaces perpendicular to the heat flux direction, which is the main contributor for thermal resistance.

4 Conclusion

Monte Carlo simulation was conducted to study the phonon transport in random composites made from nanoparticles of two different materials with large thermal conductivity contrast ratio. The effective thermal conductivity of nanoparticle composites was obtained based on the RVE with 1000 or more nanoparticles randomly stacked in space. The drift-scattering scheme [Jeng et al (2008), Mazumder and Majumdar (2001)] previously employed to simulate phonon transport in nanostructured materials were simplified and improved to render the simulation feasible for ran-

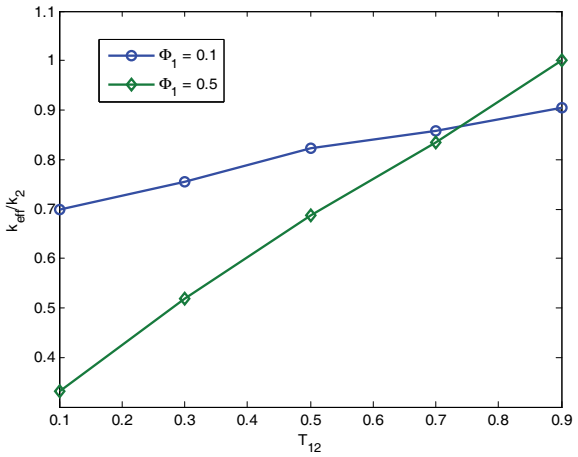

Figure 6: Effect of the phonon-interface transmissivity on the nondimensionalized effective thermal conductivity of the nanocomposites. $\Lambda_1 : \Lambda_2 : a = 100 : 1 : 1$ is used in this simulation. The interface scattering is assumed to be diffusive. The interface transmissivity is varied by changing the adjustable constant C in equation (17). Due to higher interface density, the effect of interface transmissivity is more significant for $\Phi_1 = 0.5$ than $\Phi_1 = 0.1$.

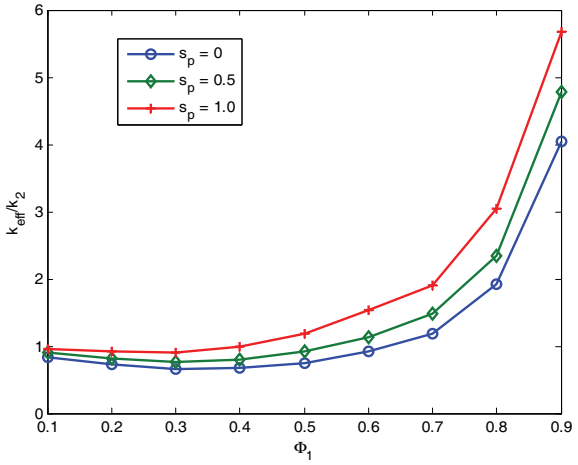

Figure 7: Effect of the specularity of phonon-interface scattering on the nondimensionalized effective thermal conductivity of nanoparticle composites. $\Lambda_1 : \Lambda_2 : a = 100 : 1 : 1$ is used in this simulation. The thermal conductivity of nanoparticle composites moderately increases with increasing the specularity because the interfaces parallel to the heat flux direction do not introduce thermal resistance when the reflection is specular.

dom nanoparticle composites studied. For the constituents with large thermal conductivity contrast ratio, we examined the effects of interface scattering on thermal conductivity percolation of random nanoparticle composites. Due to interface scattering, the geometrical percolating network formed by the high thermal conductivity particles was found not effective for the thermal conductivity improvement of nanocomposites when the nanoparticle size is comparable or smaller than the phonon mean free path of the high thermal conductivity constituent. Because the dominance of the phonon-interface scattering, the minimum thermal conductivity for composites made from small nanoparticles (particle size smaller than the phonon mean free path of both materials) occurs when the volumetric concentration of high thermal conductivity constituent is around 0.5. This lack of thermal conductivity percolation may be beneficial for improving the ratio of the electrical and thermal conductivity and thermoelectric applications beyond the percolation threshold in nanoparticle composites, because previous experiments demonstrated electrical conductivity percolation in nanocomposites, albeit different percolation thresholds and conductivity exponents from conventional percolation theory. Increasing the thermal conductivity contrast ratio improves the thermal conductivity of the composites only when the volumetric concentration of the high thermal conductivity constituents is large. This effect can saturate with further increasing the contrast ratio having no effect on the composite thermal conductivity because the dominance of interface scattering. The effective thermal conductivity of the nanoparticle composites was found to moderately increase with the transmissivity and specularity of the interface scattering.

Acknowledgement: Funding support for this work by DoD/AFOSR MURI grant FA9550-06-1-0326 and NSF-DMI 0729520 is gratefully acknowledged. The simulation was conducted on a 24-node cluster supported by Intel Corporation and managed by Prof. Gang Chen and Mr. Lu Hu at MIT. We also would like to thank Dr. Vinod Tewary for inviting the submission of this paper.

References

Abdurakhmanov, U.; Sharipov, S.; Rakhimova, Y.; Karabaeva, M.; Baydjanov, M. (2006): Conductivity and permittivity of nickel-nanoparticle-containing ceramic materials in the vicinity of percolation threshold. *J. Am. Ceram. Soc.*, vol. 89, pp. 2946-2948

Berber, S.; Kwon, Y.-K.; Tomanek, D. (2000): Unusually high thermal conductivity of carbon nanotubes. *Phys. Rev. Lett.*, vol. 84, pp. 4613-4616

Biercuk, M. J.; Llaguno, M. C.; Radosavljevic, M; Hyun, J. K.; Johnson, A. T.; Fischer, J. E. (2002): Carbon nanotube composites for thermal management. *Appl. Phys Lett.*, vol. 80, 2767

Brockhouse, B. N. (1959): Lattice vibrations in silicon and germanium. *Phys. Rev. Lett.*, vol. 2, pp. 256-258

Chen, G. (1998): Thermal conductivity and ballistic phonon transport in cross-plane direction of superlattices. *Phys. Rev. B*, vol. 57, 014958

Chen, G. (1999): Phonon wave effects on heat conduction in thin films. *J. Heat Transf.*, vol. 121, pp. 945-953

Chen, G. (2005): *Nanoscale Energy Transport and Conversion,* Oxford, New York

Dames, C.; Chen, G. (2004): Theoretical phonon thermal conductivity of Si/Ge superlattice nanowires. *J. Appl. Phys.*, vol. 95, pp. 682-693

Devpura, A; Phelan, P. E.; Prasher, R. S. (2001): Size effects on the thermal conductivity of polymers laden with highly conductive filler particles. *Microscale Therm Eng*, vol. 5, pp. 177-189

Dresselhaus, M. S.; Chen, G.; Tang, M. Y.; Yang, R. G.; Lee, H.; Wang, D. Z.; Ren, Z. F.; Fleurial, J. P.; Gogna, P. (2007): New directions for low-dimensional thermoelectric materials. *Adv. Mater.*, vol. 19, pp. 1043-1053

Drugan, W. J.; Willis, J. R. (1996): A micromechanics-based nonlocal constitutive equation and estimates of representative volume element size for elastic composites. *J. Mech. Phys. Solids*, vol. 44, pp. 497-524

Duong, H. M.; Papavassiliou, D. V.; Lee, L. L.;

Mullen, K. J. (2005): Random walks in nanotube composites: Improved algorithms and the role of thermal boundary resistance. *Appl. Phys. Lett.*, vol. 87, 013101

Dubson, M. A.; Garland, J. C. (1985): Measurement of the conductivity exponent in two-dimensional percolating networks: square lattice versus random-void continuum. *Phys. Rev. B*, vol. 11, pp. 7621-7623

Foygel, S; Morris, R. D.; Anez., D.; French, S.; Sobolev, V. L. (2005): Theoretical and computational studies of carbon nanotube composites and suspensions: Electrical and thermal conductivity. *Phys. Rev. B*, vol. 71, 104201

Ganapathy, D; Singh, K.; Phelan, P. E.; Prasher, R. (2005): An effective unit cell approach to compute the thermal conductivity of composites with cylindrical particles. *J. Heat Transf.*, vol. 127, pp. 553-559

Gerenrot, D.; Beryand, J; Phillips, J (2003): Random network model for heat transfer in high contrast composite materials. *IEEE Trans. Adv. Pack.*, vol. 26, pp. 410-416

Goldsmid, H. J. (1964): *Thermoelectric Refrigeration*, Plenum Press, New York

Gonon, G.; Boudefel, A. (2006): Electrical properties of epoxy/silver nanocomposites. *J. Appl. Phys.*, vol. 99 024308

Heremans, J. P.; Thrush, C. M.; Morelli, D. T. (2005): Thermopower enhancement in PbTe with Pb precipitates. *J. Appl. Phys.*, vol. 98, 063703

Hirano, T.; Izaki, K.; Niihara, K. (1995): Microstructure and thermal conductivity of Si3N4/SiC nanocomposites fabricated from amorphous Si-C-N precursor powders. Nanostruct. Mater., vol. 5, pp. 809-818

Hone, J.; Whitney, M.; Piskoti, C.; Zettl, A. (1999): Thermal conductivity of single-walled carbon nanotubes. *Phys. Rev. B*, vol. 59, R2514

Hsu, K. F.; Loo, S.; Guo, F.; Chen, W.; Dyck, J. S.; Uher, C.; Hogan, T.; Polychomiadis, E. K.; Kanatzidis, M. G. (2004): Cubic AgPbmSbTe2+m: Bulk thermoelectric materials with high figure of merit. *Science*, vol. 303, pp. 818-821

Hu, X.; Jiang, L.; Goodson, K. E. (2004): Thermal conductance enhancement of particle-filled thermal interface materials using carbon nanotube inclusions. *Proceedings of Inter Society Conference on Thermal Phenomena*, pp. 63-69

Huang, H; Liu, C.; Wu, Y.; Fan, S. (2005): Aligned carbon nanotube composite films for thermal management. *Adv. Mater.*, vol. 17, pp. 1652-1656

Jeng, M. S.; Yang, R. G.; Song, D.; Chen, G. (2008): Modeling the thermal conductivity and phonon transport in nanoparticle composites using Monte Carlo simulation. *J. Heat Transf.*, in press

Kanit, T.; Forest, S.; Galliet, I.; Mounoury V.; Jeulin, D. (2003): Determination of the size of the representative volume element for random composites: statistical and numerical approach. *Int. J. Solids Struct.*, vol. 40, pp. 3647-3679

Kim, P.; Shi, L.; Majumdar, A.; McEuen, P. L. (2001): Thermal transport measurements of individual multiwalled nanotubes. *Phys. Rev. Lett.*, vol. 87, 215502

Kirkpatrick, S. (1973): Percolation and conduction. *Rev. Mod. Phys.,* vol. 45, pp. 574-588

Kittel, C. (1986): *Introduction to Solid State Physics*, John Wiley & Sons, New York

Kumar, S.; Alam, M. A.; Murthy, J. Y. (2007): Effect of percolation on thermal transport in nanotube composites. *Appl. Phys. Lett.*, vol. 90, 104105

Kusunose, T; Kim, Y.-H.; Sekino, T.; Matsumoto, T. (2005): Fabrication of Al_2O_3/BN nanocomposites by chemical processing and their mechanical properties. *J. Mater. Res.*, vol. 20, pp. 183-190

Last, B. J.; Thouless, D. J. (1971): Percolation theory and electrical conductivity. *Phys. Rev. Lett.*, vol. 27, pp. 1719-1721

Liang, X.-G.; Ji, X. (2000): Thermal conductance of randomly oriented composites of thin layers. *Int. J. Heat Mass Transf.*, vol. 43, pp. 3633-3640

Lacroix, D.; Joulain, K.; Lemonnier, D. (2005): Monte Carlo transient phonon transport in silicon and germanium at nanoscales. *Phys. Rev. B*, vol.

72, 064305

Lüscher, M. (1994): A portable high-quality random number generator for lattice field theory simulations. *Comput. Phys. Commun.*, vol. 79, pp. 100-110

Majumdar, A. (1993): Microscale heat conduction in dielectric thin films. *J. Heat. Transf.*, vol. 115, pp. 7-16

Mamunya, Y. P.; Davydenko, V. V.; Pissis, P.; Lebedev, E. V. (2002): Electrical and thermal conductivity of polymers filled with metal powders. *Eur. Polym. J.*, vol. 38, pp. 1887-1897

Mayrhofer, P. H.; Willmann, H.; Mitterer, C. (2003): Recrystallization and grain growth of nanocomposite Ti–B–N coatings. *Thin Solid Films*, vol. 440, pp. 174-179

Mazumder, S.; Majumdar, A. (2001): Monte Carlo study of phonon transport in solid thin films including dispersion and polarization. *J. Heat. Transf.*, vol. 123, pp. 749-759

Namilae, S.; Chandra, U.; Srinivasan, A.; Chandra, N. (2007): Effect of interface modification on the mechanical behavior of carbon nanotube reinforced composites using parallel molecular dynamics simulations. *CMES: Computer Modeling in Engineering and Sciences*, vol. 22, pp. 189-202

Nan, C-W; Liu, G.; Lin, Y.; Li, M. (2004): Interface effect on thermal conductivity of carbon nanotube composites. *Appl. Phys. Lett.*, vol. 85, 3549

Okada, H.; Fukui, Y.; Kumazawa, N. (2004): Homogenization analysis for particulate composite materials using the boundary element method. *CMES: Computer Modeling in Engineering and Sciences*, vol. 5, pp. 135-150

Oregan, B.; Gratzel, M. (1991): A low-cost, high-efficiency solar cell based on dye-sensitized colloidal TiO_2 films. *Nature*, vol. 353, pp. 737-740

Pop, E.; Mann, D.; Wang, Q.; Goodson, K.; Dai, H. (2006): Thermal conductance of an individual single-wall carbon nanotube above room temperature. *Nano Lett.*, vol. 6, pp. 96-100

Prasher, R. (2006): Thermal conductivity of tubular and core/shell nanowires. *Appl. Phys. Lett.*, vol. 89**,** 063121

Ren, Z. Y.; Zheng, Q. S. (2002): A Quantitative study of minimum sizes of representative volume elements of cubic polycrystals—numerical experiments. *J. Mech. Phys. Solids*, vol. 50, pp. 881-893

Shenogina, N.; Shenogin, S.; Xue, L.; Keblinski, P. (2005): On the lack of thermal percolation in carbon nanotube composites. *Appl. Phys. Lett.*, vol. 87, 133106

Stauffer, D.; Aharony, A. (1991): *Introduction to Percolation Theory*, 2nd ed., Taylor & Francis, London.

Swartz, E. T.; Pohl, R. O. (1989): Thermal boundary resistance. *Rev. Mod. Phys.*, vol. 61, pp. 605-668

Thovert, J. F.; Wary, F.; Adler, P. M (1990): Thermal conductivity of random media and regular fractal. *J. Appl. Phys.*, vol. 68, pp. 3872-3883.

Tian, W.; Yang, R. G. (2007a): Thermal conductivity modeling of compacted nanowire composites. *J. Appl. Phys.* vol. 101, 054320

Tian, W.; Yang, R. G. (2007b): Effect of interface scattering on phonon thermal conductivity percolation in random nanowire composites. *Appl. Phys. Lett.*, vol. 90, 263105

Tritt, T. M.; Subramanian, M. A. (editors) (2006): *Harvesting Energy through Thermoelectrics: Power Generation and Cooling*, MRS Bull vol. 31, No. 3, the whole theme issue on thermoelectrics

Wang, H.; Yao, Z. (2005): A new fast multipole boundary element method for large scale analysis of mechanical properties in 3D particle-reinforced composites. *CMES: Computer Modeling in Engineering and Sciences*, vol. 7, pp. 85-96

Xu, J.; Fisher, T. S. (2006): Enhancement of thermal interface materials with carbon nanotube arrays. *Int. J. Heat Mass Transf.*, vol. 49, pp. 1658-1666

Yamamuro, S.; Sumiyama, K.; Hihara, T; Suzuki, K. (1999): Geometrical and electrical percolation in nanometre-sized Co-cluster assemblies. *J. Phys.: Condens. Matter.*, vol. 11, pp.

3247-3257

Yang, R. G; Chen, G (2004): Thermal conductivity modeling of periodic two-dimensional nanocomposites. *Phys. Rev. B*, vol. 69, 195316.

Yang, R. G; Chen, G; Dresselhaus, M. S. (2005): Thermal conductivity of simple and tubular nanowire composites in the longitudinal direction. *Phys. Rev. B*, vol. 72, 125418

Zhan, G.-D.; Kuntz, J; Wan, J.; Garay, J.; Mukherjee, A. K. (2003): Spark-plasma-sintered $BaTiO_3/Al_2O_3$ nanocomposites. *Mat. Sci. Eng. A-Struct.*, vol. A356, pp. 443-446